Massive mudstones in basin analysis and paleoclimatic interpretation of the Newark Supergroup

JOSEPH P. SMOOT and PAUL E. OLSEN

ABSTRACT

Massive red or gray mudstones, which occur at the tops of 2- to 10-m-thick sedimentary cycles, constitute a large portion of the Newark Supergroup. The mudstones can be separated into four distinct types; each type can be related to a specific set of paleoenvironmental conditions through analogy to modern sedimentary environments. *Mud-cracked massive mudstone*, dominated by narrow, jagged polygonal cracks and millimeter-scale, cement-filled vugs, is interpreted as subaerial, playa mud-flat deposits. *Burrowed massive mudstone*, dominated by sediment-filled tubes having constant diameters and commonly containing soft-sediment deformation features, deep, narrow mud cracks, and lacustrine fossils, is interpreted as intermittently exposed shallow lake or swampy flood-plain deposits. *Root-disrupted massive mudstone*, dominated by small, cement-filled tubes that taper and bifurcate and containing mud cracks, syndepositional carbonate nodules, and burrows, is interpreted as vegetated flood-plain, lake-margin, or overbank deposits with soil development. *Sand-patch massive mudstone*, characterized by irregularly shaped pods of sandstone and siltstone that have angular to cuspate margins, internal zones of different grain sizes, and jagged internal cracks and commonly containing evaporite crystal molds, is interpreted as the deposits of a saline mud flat.

Mud-cracked massive mudstone and sand-patch massive mudstone occur only in the northern Newark basins, while burrowed massive mudstone and root-disrupted massive mudstone dominate in the southern basins but also occur within certain stratigraphic intervals within the northern basins. These occurrences suggest that paleolatitude limited arid conditions to the northern basins and that temporal changes in paleoclimate were also important. If there were unique depositional periods of dry versus wet conditions, they may be used as chronostratigraphic markers for correlation between basins and across lithologies within basins.

Introduction

The Newark Supergroup is composed of Late Triassic to Early Jurassic continental sedimentary rocks and interbedded basalts that crop out in a series of elongated basins along the eastern margin of North America (Fig. 10-1; Froelich and Olsen, 1985). The Newark Supergroup basins are interpreted as half-grabens formed by extension related to the opening of the Atlantic Ocean. The sedimentary deposits of these basins are commonly compared to those of modern rift valleys, such as the East African rift valleys, and to the Basin and Range province of the western United States (Reinemund, 1955; Van Houten, 1962, 1964; Hubert et al., 1976; Bain and Harvey, 1977; Hubert and Hyde, 1982; Robbins, 1982; Gore, 1983, 1986; Hentz, 1985; LeTourneau, 1985; among many others). Most depositional models call for alluvial fans along fault margins grading basinward into lacustrine shales and mudstones or into fluvial channel sandstones and flood-plain mudstones. The paleodrainages are generally interpreted as being closed with a bullseye pattern of fluvial deposits surrounding the lacustrine deposits, but some basins may have had through-going drainages at least during part of their depositional histories (Smoot, 1985).

The typically cyclic lacustrine shales and mudstones in the Newark Supergroup reflect the rise and fall of lake level apparently in response to climatic changes (Van Houten, 1962, 1964; Olsen, 1986). These lacustrine cycles, termed 'Van Houten Cycles' by Olsen (1985), consist of gradational sequences of (1) thin-bedded silty mudstone having polygonal cracks or sandstone having oscillatory ripples, which reflect shallow lake deposition, (2) a middle section ranging from very finely laminated, organic-rich, black shale to thin-bedded gray mudstone, which reflects deeper water deposition, and (3) an upper massive mudstone or interbedded

EXPLANATION

1. Wadesboro (N.C.–S.C.)
2. Deep River (N.C.)
3. Durham (N.C.)
4. Davie County (N.C.)
5. Dan River and
   Danville (N.C.–Va.)
6. Scottsburg (Va.)
7. Basins north of
   Scottsburg (Va.)
8. Farmville (Va.)
9. Richmond (Va.)
10. Taylorsville (Va.)
11. Scottsville (Va.)
12. Barboursville (Va.)
13. Culpeper (Va.–Md.)
14. Gettysburg (Md.–Pa.)
15. Newark (N.J.–Pa.–N.Y.)
16. Pomperaug (Conn.)
17. Hartford (Conn.–Mass.)
18. Deerfield (Mass.)
19. Fundy or Minas
    (Nova Scotia–Canada)
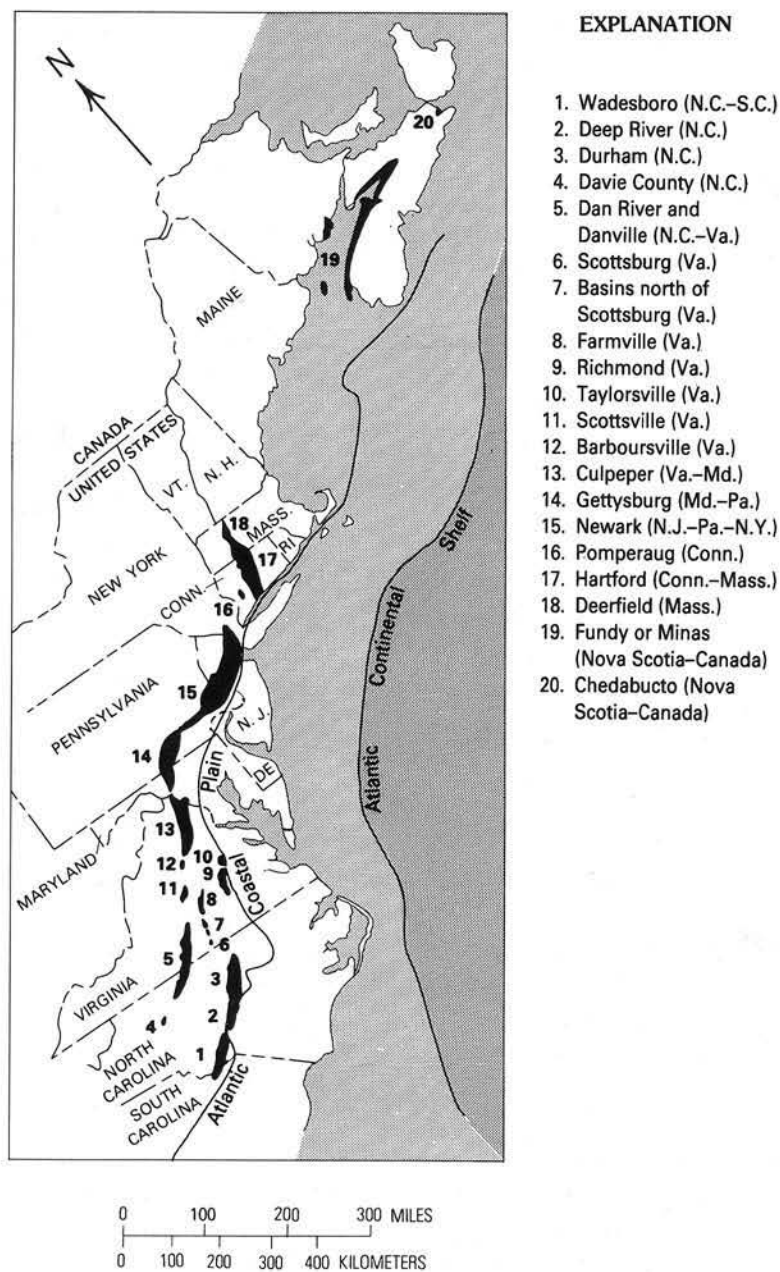20. Chedabucto (Nova
    Scotia–Canada)

Fig. 10-1. Exposed basins of the Newark Supergroup in eastern North America (black areas). From Froelich and Olsen (1985).

sandstone and mudstone commonly containing mud cracks and root casts, which reflects shallow-water deposition to subaerial deposits. Variations on the cyclic theme include thin-bedded, mud-cracked mudstone grading upward into massive mudstone or, near the margins of basins, laminated black shale or thin-bedded, gray mudstone grading upward into sandstone or conglomerate shoreline and fluvial deposits. Although some of the vertical changes in cycles may be due to aggradation, such as by river bar migration or delta progradation, many of the characteristics are better explained by changes in lake depth (Van Houten, 1962, 1964; Olsen, 1980b, 1986). The rise of lake level is believed to be a response to increased fluvial input into the basins during periods of higher net precipitation. Therefore, the mudstones and sandstones at the cycle tops represent the periods of lowest inflow into the basins or the driest conditions.

Massive red or gray mudstones, which comprise the tops of lacustrine cycles or which are interbedded with fluvial sandstones, make up a large portion of the fine-grained sedimentary rocks of the Newark Supergroup. Despite their presence in every Newark Supergroup basin and their volumetric dominance in the ubiquitous lacustrine cycles, massive mudstones have not been adequately studied or described compared to conglomerates, sandstones, and laminated or thin-bedded siltstones, claystones, and limestones. Presumably, the lack of massive mudstone studies are due to the difficulty in making textural descriptions of outcrops and to the dearth of depositional models. The widespread distribution of massive mudstones and their facies associations within the Newark Supergroup basins suggest that they may be useful in stratigraphic basin analysis. Furthermore, massive mudstones have distinctive textures that are indicative of degree of desiccation or water saturation. The distribution of these distinctive features suggest that massive mudstones may be used for paleoclimatic interpretation, especially in the context of their surrounding facies.

We should note that we are using the term massive mudstone in a broad sense, encompassing rocks that tend to have a blocky or hackly appearance on a weathered outcrop and that show little obvious internal structure on superficial examination. These same mudstones may show considerable internal structure when viewed on a cut surface, including remnant layering. Mudstones showing absolutely no internal structure are very uncommon in the Newark Supergroup.

Types of massive mudstones

We recognize four major types of massive mudstone textures in the Newark Supergroup: (1) *mud-cracked massive mudstone;* (2) *burrowed massive mudstone;* (3) *root-disrupted massive mudstone;* and (4) *sand-patch massive mudstone* (Smoot and Olsen, 1985). Gradations exist between each of these mudstone types; therefore, each is treated as an end-member having dominant, distinctive fabrics and particular associated sedimentary features. Our interpretations of the massive mudstones are largely based on direct comparison to modern deposits. These interpretations are further constrained by the associated sedimentary features within cycles (Fig. 10-2).

Although many of the massive mudstones contain fabrics similar to those formed in soils, such as oriented clay coatings, synsedimentary slickensides, root structures, and carbonate nodules, we will not use soil classification terms as in Retallack (1977). Many of the criteria used to differentiate paleosol type (for instance, Retallack, 1977; Bown and Kraus, 1981; Blodgett, 1984) are often not applicable to the Newark examples due to diagenetic overprints such as hematite and dolomite crystal growth and recrystallization of clays.
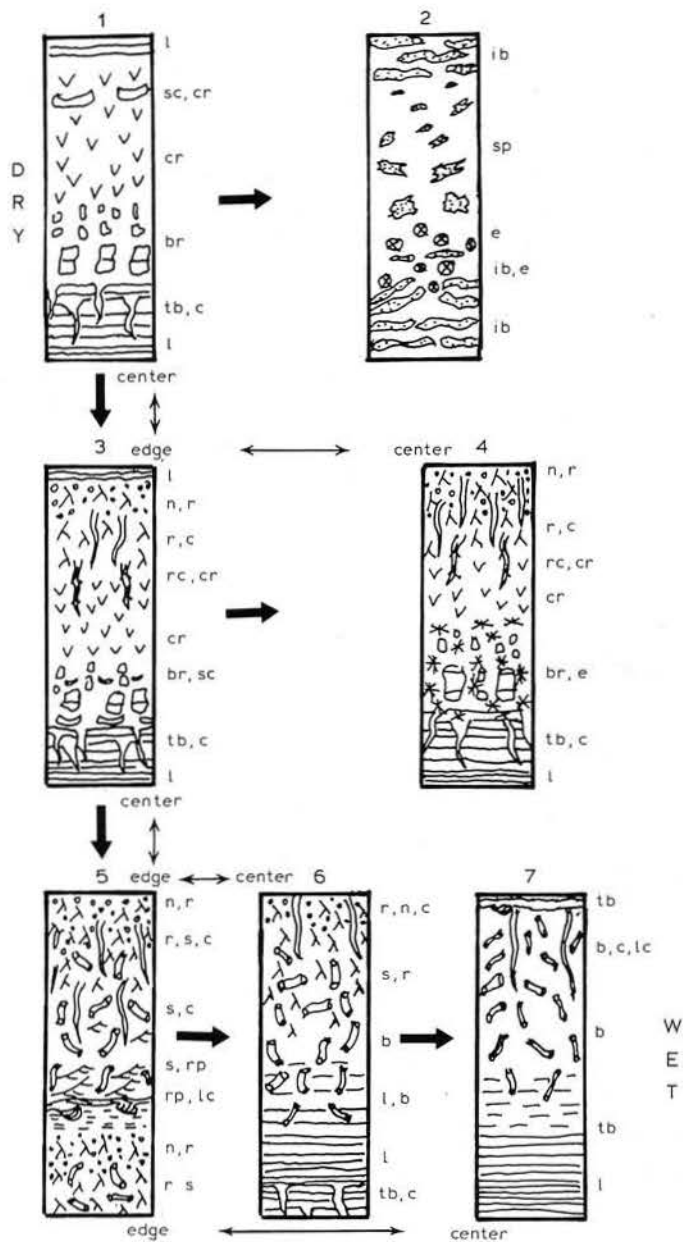
Fig. 10-2. Schematic drawing of sedimentary sequences containing massive mudstones (after Smoot and Olsen, 1985). Thick arrows show interpretations of relative degrees of dryness or wetness in the depositional environments of sequences. The driest sequence is at upper left and the wettest is at lower right. Thinner arrows show possible geographic relationships between sequences within a basin. Sequence 1 is 3 – 5 m thick; sequence 2 is 1 – 3 m thick; sequence 3 and 4 are 3 – 7 m thick, sequence 5 is 6 – 20 m thick; sequences 6 and 7 are 6 – 30 m thick. Symbols: b = burrows; br = breccia fabric; c = cracks; cr = crumb fabric; e = evaporite molds; ib = irregular bedding; l = flat lamination; lc = load casts; n = carbonate nodules; r = root structures; rc = roots within cracks; rp = ripple cross-laminae; s = *Scoyenia*; sc = silt curls; sp = sand-patch fabric; tb = thin bedding.

Mud-cracked massive mudstone

Mud-cracked massive mudstone is characterized by abundant small (1 – 5 cm deep), narrow, jagged cracks or sinuous cracks having indistinct edges, both of which form a polygonal pattern in plan view (Fig. 10-3). The cracks are commonly filled with more mudstone or with sandstone. Broad cracks may have complex, cross-cutting, or stratified fillings, and narrow cracks may be filled with cements including calcite, dolomite, albite, or analcime. Varying proportions of two different fabrics of mud-cracked massive mudstone are often present – a breccia fabric and a crumb fabric (Fig. 10-2). The breccia fabric is defined by polygonal cracks that separate blocks of mudstone (Fig. 10-4). Mudstone blocks that are internally thin bedded show no evidence of displacement or rotation (e.g., Van Houten, 1964, Figs. 8, 12, and 13; Katz, 1983). Curved, slickensided planes that offset cracks in a complex pattern of superimposed bowl-shaped polygons (e.g., Van Houten, 1964, fig. 14) are also common in the breccia fabric. The crumb fabric typically gradationally overlies the breccia fabric. The crumb fabric has narrower cracks forming smaller polygons than the breccia fabric and is comprised of millimeter-scale mud clumps and abundant laminoid and ovoid, cement-filled
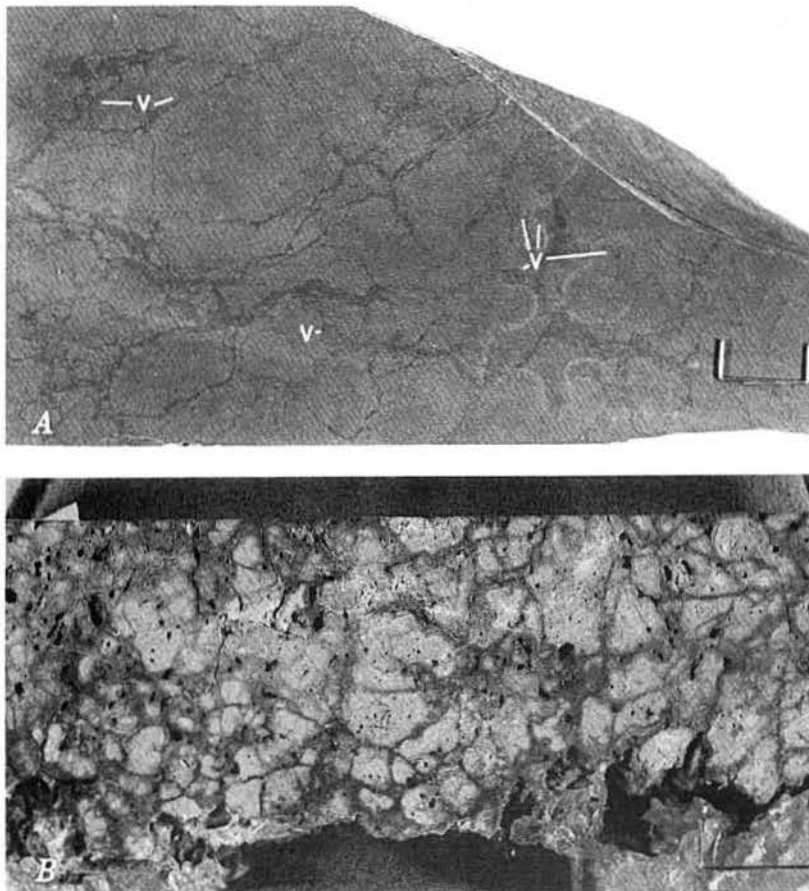

Fig. 10-3. Plan-view slabs of (A) mud-cracked massive mudstone, Balls Bluff Siltstone near Culpeper, Virginia, and (B) plastic-impregnated modern mud from mud-cracked playa surface, Mud Lake, Nevada. Narrow, clay-filled cracks define centimeter-scale polygons. Circular cross sections in A are interpreted as clay-filled vesicles (*v*), open vesicles in B appear black. Staples are 7 mm long.

vugs (Fig. 10-5A) that also commonly have thin clay linings (Katz, 1983). The cracks in the crumb fabric may by sinuous and have indistinct cross sections. Some occurrences of crumb fabric do not have the cement-filled vugs, but small clay blebs may be compacted clay-lined vugs (see Demicco and Kordesch, 1986).

Mud-cracked massive mudstone gradationally overlies laminated to thin-bedded, lacustrine mudstone having large polygonal cracks, conchostracans, ostracodes, and rare reptile footprints and other ichnofossils (Fig. 10-2, sequences 1, 3, and 4). The massive mudstone commonly contains centimeter-scale siltstone beds that form concave-upward polygonal curls, and thin, muddy sandstone lenses having scoured bases. Cement-filled pseudomorphs after a bladed evaporite mineral, possibly gypsum, have been found in a few occurrences of brecciated mudstone (Fig. 10-6). Some of the cement-filled vugs and cracks have also been interpreted as evaporite pseudomorphs (Van Houten, 1965).

Mud-cracked massive mudstones that have the breccia fabric are interpreted as lacustrine beds that were disrupted by repeated desiccation and rewetting over long periods of very slow deposition, by analogy to processes occurring on modern playa flats (Smoot, 1981; Smoot and Katz, 1982). The blocks of mudstone are lake deposits displaced by superimposed polygonal cracks that were infilled with sediment during flooding events, then recracked, while no new sedimentary layers were deposited. The slickenside planes probably formed by the expansion and contraction of the fine-grained lake clays under these conditions.

Mud-cracked massive mudstone with a crumb fabric matches modern basin floor deposits of aggrading playa mud flats (Smoot and Katz, 1982; Katz, 1983). The conditions of formation are the same as for the breccia fabric, but the layers disrupted by the superimposed mud cracks are irregular, discontinuous submillimeter laminae of silty mud having trapped air bubbles (Fig. 10-5B). Cracks that are not completely filled with sediment during floods
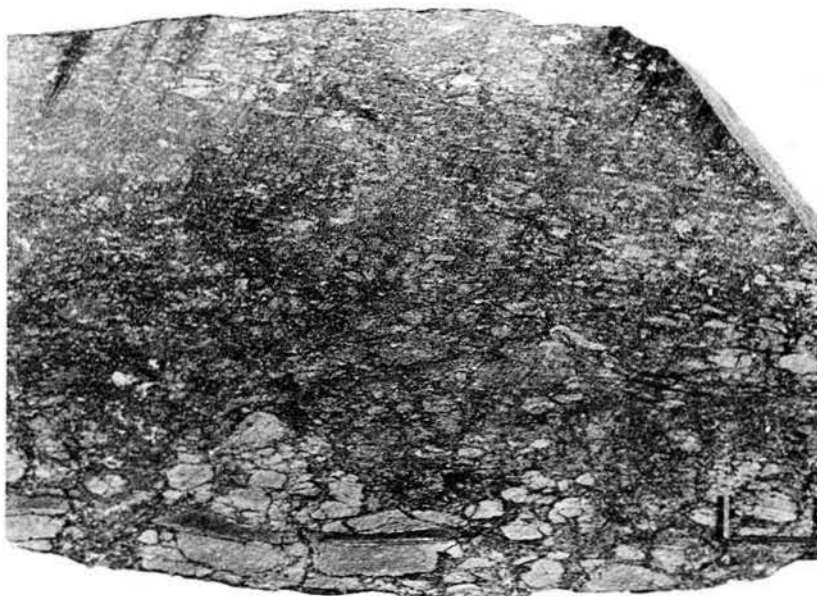

Fig. 10-4. Cross-section slab of breccia fabric in mud-cracked massive mudstone, Balls Bluff Siltstone near Culpeper, Virginia. Light gray patches are greenish claystone; dark gray areas are red, silty mudstone filling polygonal cracks in plan view. Note the layering in adjacent clumps near the base of the sample and the zone of light gray clumps at the top reflecting original layering. Staple is 7 mm long.

become distorted when resaturated due to collapse and flowage. The air bubbles produce a vesicular fabric that is identical to the cement-filled vugs in the mud-cracked massive mudstone. Rain splash and small-scale flooding during the long periods between deposition cause eluviation of clays and the formation of clay coats around the open vesicles and cracks. The preservation of silt layers disrupted into polygons by desiccation and of undisturbed sand lenses within the crumb fabric indicate that it is aggradational rather than degrada-
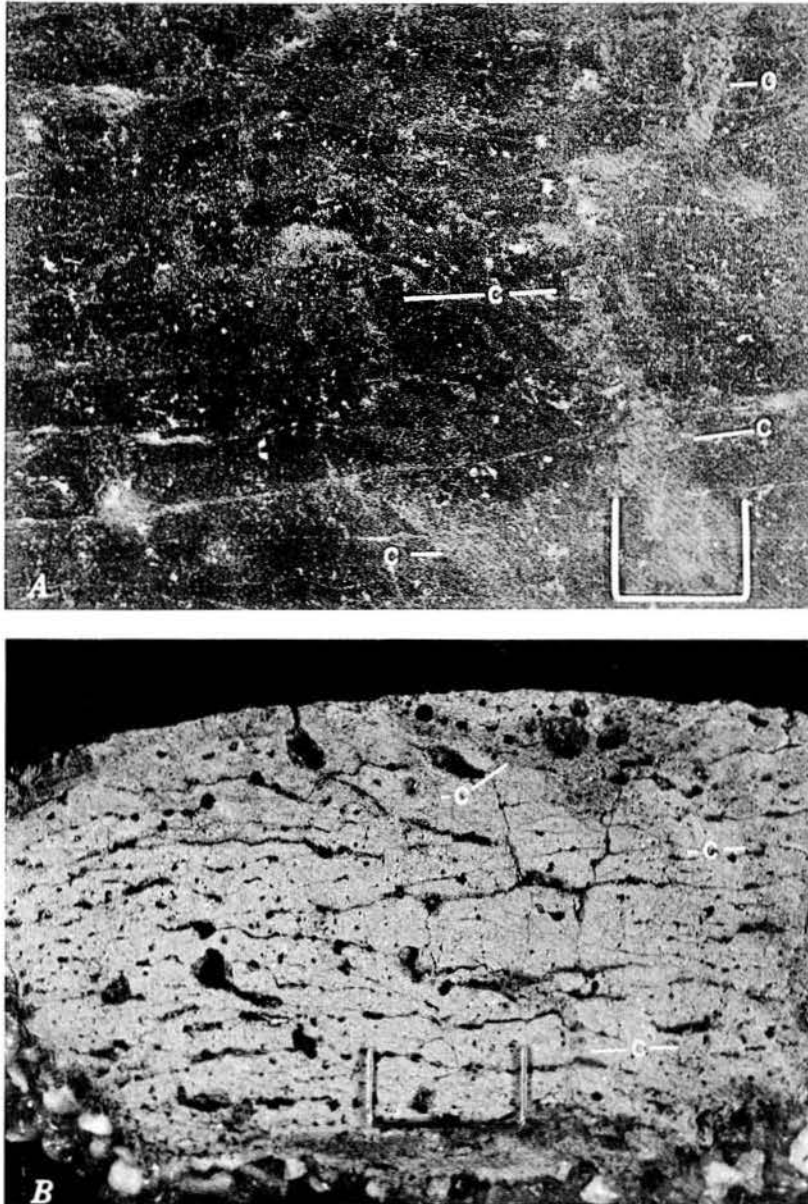

Fig. 10-5. Cross-section slabs of (A) crumb fabric in mud-cracked massive mudstone, Lockatong Formation near Frenchtown, New Jersey, and (B) plastic-impregnated modern mud from the mud-cracked playa surface of Mud Lake, Nevada. Sediment-filled mud cracks (c) have distorted margins. Irregular ovoid and horizontally elongated light-gray and white patches in 5A are clay and dolomite and analcime cements that are interpreted as equivalents to the vesicles in B (black). Staple in A is 6 mm long, and staple in B is 7 mm long.

Fig. 10-6. Cross section of evaporite crystal molds in the transition from thin-bedded, mud-cracked mudstone to mud-cracked massive mudstone. The area marked by arrows is a dome-shaped mass of radiating crystal molds (gypsum?) in a mudstone matrix. Discrete vertical splays of crystal molds (S) occur below the dome-shaped mass and crystal masses restricted to cracks (C) occur above the dome-shaped mass. The top of the sample consists of the crumb fabric having tiny subhedral to anhedral crystal molds. Staple is 6 mm long.

tional. The common occurrences of virtually uncompacted, cement-filled vesicles and cracks in the mud-cracked massive mudstone suggest that at least some cementation occurred before burial.

Burrowed massive mudstone

Burrowed massive mudstone is dominated by 0.5 – 1.0-cm diameter tubes that commonly show no preferred orientation, have constant diameters, and are filled with mudstone or sandstone. These tubes are interpreted as burrows. The most distinctive types of tubes are *Scoyenia* (Olsen, 1977), which are characterized by spreiten (curved, meniscus-type laminae, defined by small grain size changes, oriented perpendicular to the wall of the tube) (Fig. 10-7) and rice grain textured outer walls, the latter only visible in very fine-grained units. Other kinds of tubes having simple fillings and smooth walls are commonly present and may be dominant (Fig. 10-8). Burrows may be so abundant as to obscure the individual cross sections and produce a mottled texture (Fig. 10-9). The mottling has distinctive ovate or arcuate patches reflecting the outlines of burrows. Burrowed massive mudstones commonly contain a minor component of small, often submillimeter flattened tubes, which bifurcate and taper. We interpret these tubes as the casts and molds of roots (see below). Large, 10 – 20-centimeter deep polygonal cracks and scattered carbonate nodules may be present in these mudstones, and relict patches of sedimentary layering are common (Fig. 10-8).

Burrowed massive mudstones are associated with two types of sequences. The most common association is with fine-grained, micaceous sandstones having climbing-ripple cross-

lamination and soft-sediment deformation including load casts, pseudonodules, and oversteepened ripple cross-laminae (Fig. 10-9A), and with laminated shales that commonly contain abundant conchostracans, ostracodes, and other aquatic fossils (Fig. 10-2, sequence
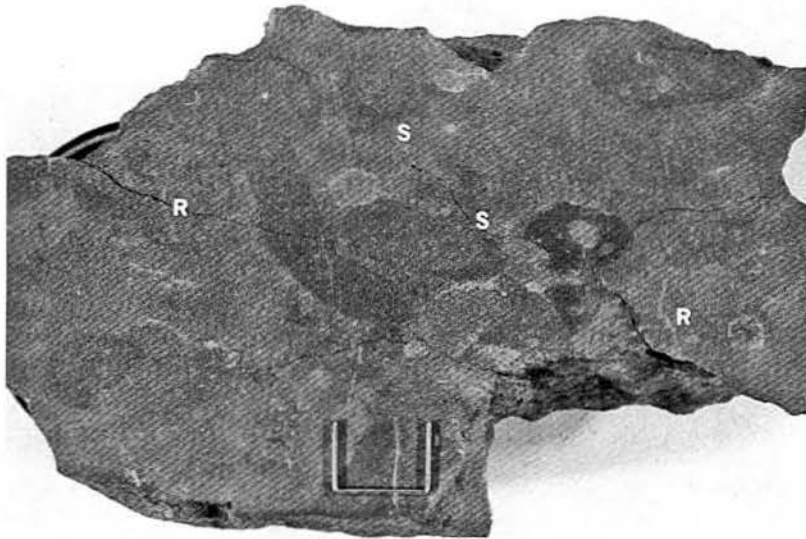

Fig. 10-7. Cross-section slab of burrowed massive mudstone that has *Scoyenia*-type burrows, Passaic Formation near Gladstone, New Jersey. Sprieten are faintly visible as light-dark arcuate boundaries (*S*). Thin, light-colored vertical streaks are calcite-filled tubes interpreted as root casts (*R*). Circular, light-colored patches are spheroidal, calcite-cemented areas that may be soil carbonates. Staple is 6 mm long.
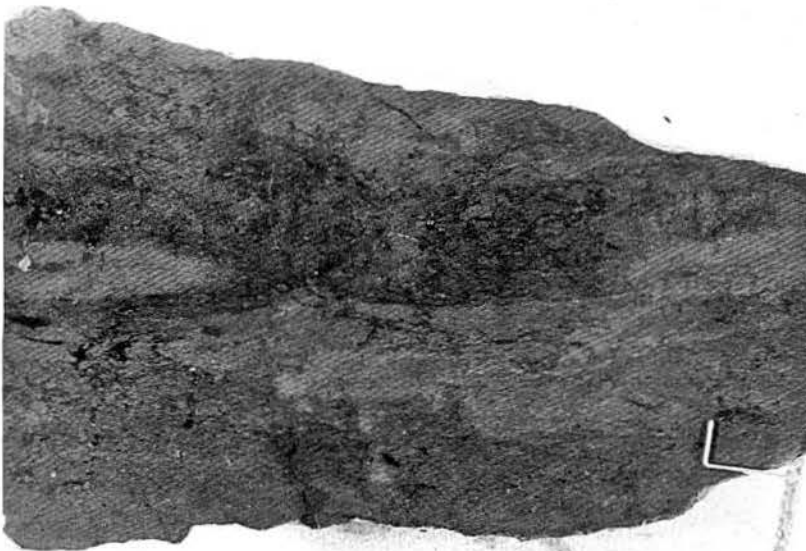

Fig. 10-8. Cross-section slab of burrowed massive mudstone, Lockatong Formation near Gwynned, New Jersey. Relict thin bedding is visible as lighter and darker bands. Disruptions are cross sections of tubes and are interpreted as burrows. Staple is 7 mm long.

5; Fig. 10-19). Reptile footprints are common on bedding planes that are not obscured by burrows, and disarticulated fish fossils and reptile bones are occasionally found. The other association is with microlaminated mudstone or limestone that grades upward into wispy thin beds then into massive mudstone by a gradual loss of layer definition (Fig. 10-2, sequences 6 and 7; Fig. 10-20), apparently due to small-scale bioturbation (Olsen, 1984, pp. 521 – 527).
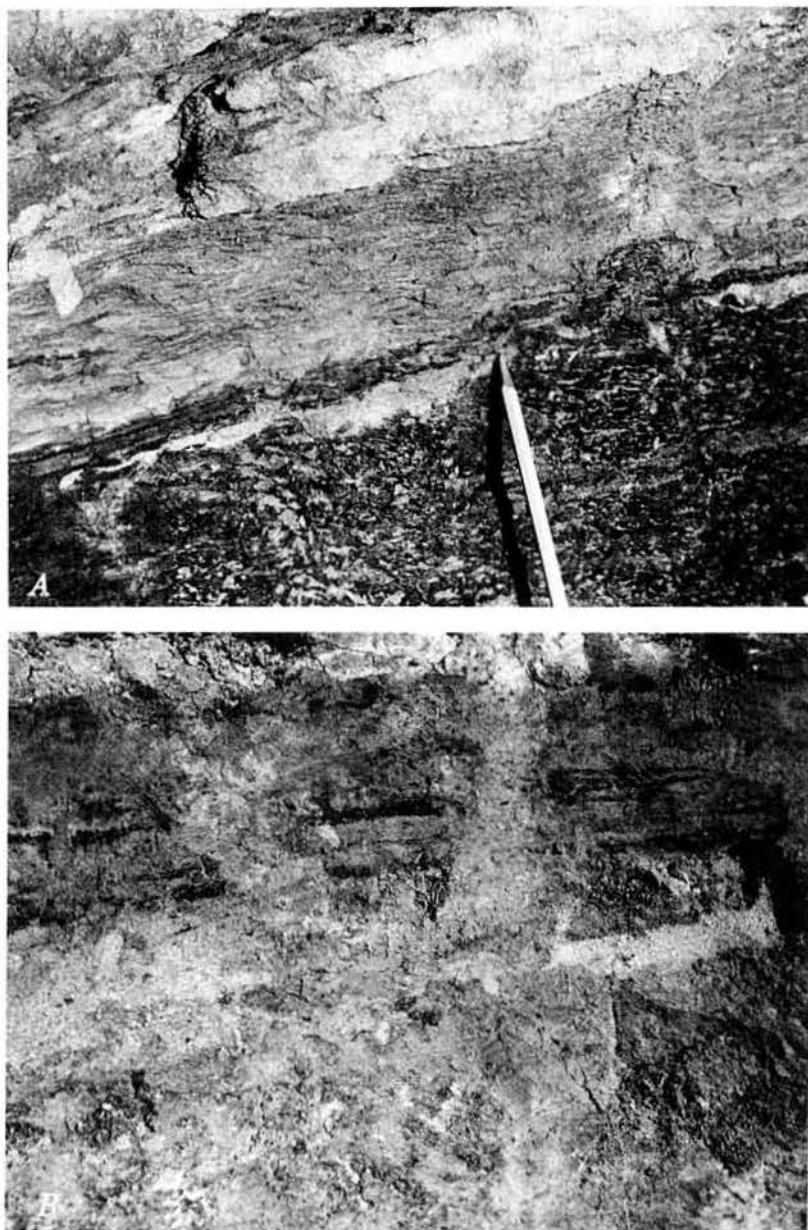

Fig. 10-9. Cross-section view of (A) outcrop of burrow-mottled mudstone having *Scoyenia*-type burrows overlain by ripple cross-laminated sandstone, Sanford Formation near Glenlee, North Carolina, and (B) trench in swampy floodplain of the Mississippi River near Marked Tree, Arkansas. Layer of ripple cross-laminated sand at top of trench overlies a mottled silty clay having abundant burrows probably formed by crayfish. Two large disruptions of the sand layer are probably due to roots. Both photos show about 25 cm of vertical section.

When clearly visible these millimeter to submillimeter burrows lack spreiten.

The burrowed massive mudstones probably represent several different depositional environments, including lake margins, delta plains, and fluvial floodplain-overbank settings (Fig. 10-9B). The makers of the burrows probably represent a wide variety of invertebrates. There is no consensus on the makers of even the distinctive and common *Scoyenia*-type burrows. Opinions range from polychaete worms or insects (Frey et al., 1984) to crayfish-like crustaceans (Olsen, 1977) despite the fact that *Scoyenia*-like burrows are known from modern deposits (Wells, 1977). The makers of the other burrows are similarly cryptic, but worms and aquatic insect larvae are plausible.

Root-disrupted massive mudstone

Root-disrupted massive mudstone is characterized by abundant downwardly bifurcating and tapering tubes, ranging in diameter from submillimeter to decimeters (Fig. 10-10). These characteristics are believed to be diagnostic of roots and root traces. The tubes are predominantly oriented perpendicular to bedding, but they may also be parallel, forming radiating patterns away from larger vertical tubes (Fig. 10-11A). Large tubes are commonly filled with sandstone or mudstone, whereas smaller tubes are commonly lined with tangentially oriented clays, which may also define the entire tube shape. Small tubes may also be filled with cement. In some cases, actual fusinite (carbonized) root remains are present, and in one case, small fusinite trees or shrubs have been found *in situ* on the surface of a root-disrupted massive mudstone.

Spherical nodules of micritic calcite and dolomite, ranging from sand-sized to several millimeters in diameter, are commonly concentrated in the larger tubes or scattered in the surrounding matrix. Sandstones associated with the root-disrupted massive mudstones commonly contain large amounts of carbonate grains having sizes and textures similar to those
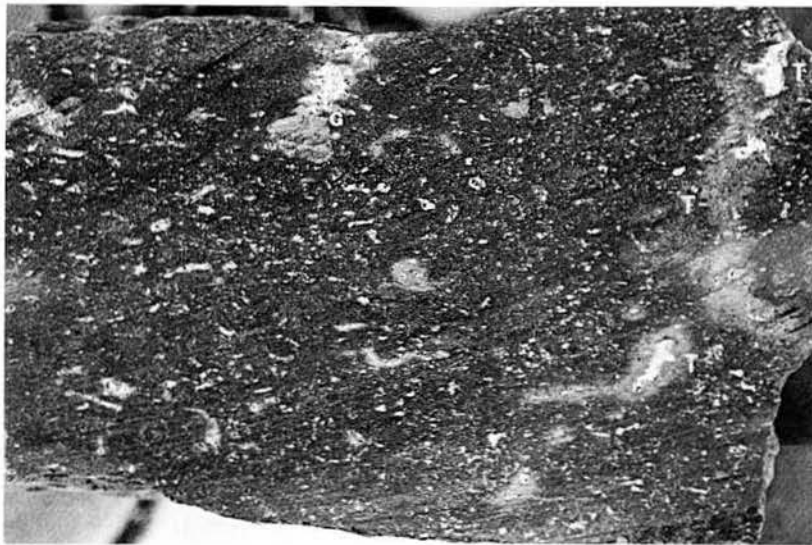

Fig. 10-10. Cross-section slab of root-disrupted massive mudstone, Passaic Formation near Neshanic Station, New Jersey. The white features are calcite-filled tubes interpreted as root casts and the gray areas are reduction halos. Vertical structure on right is a larger downward-tapering, branching tube (*T*). Sample is 7 cm thick.

of the nodules; these similarities indicate that the nodules were locally eroded and reworked. Some root-disrupted massive mudstones grade into root-disrupted limestone by coalescence of centimeter-scale nodules. *Scoyenia,* polygonal cracks (5 – 10 cm deep), and bowl-shaped slickenside planes (similar to Gray, 1984) may also occur in root-disrupted massive
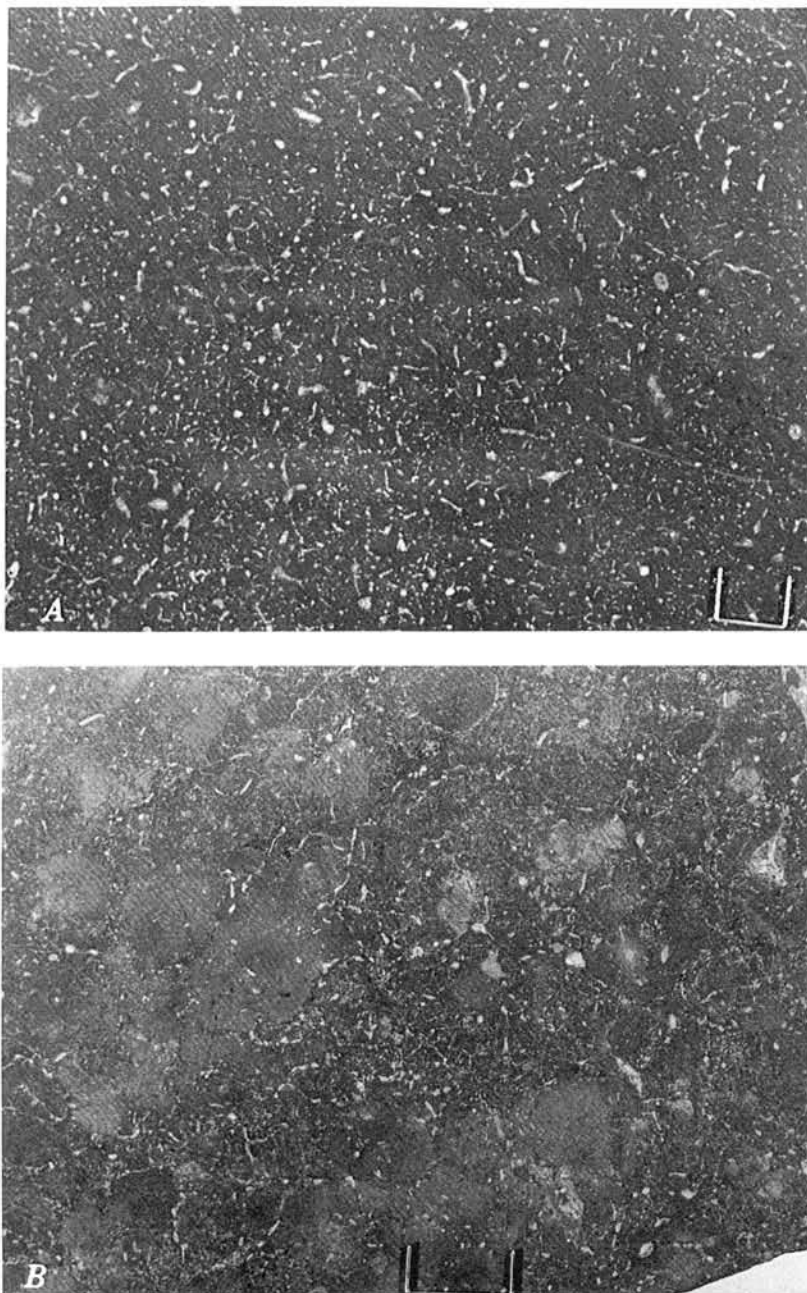

Fig. 10-11. Plan-view slabs of root-disrupted massive mudstones, Balls Bluff Siltstone near Culpeper, Virginia. A is from the top of a cycle, and B is from transition with a mud-cracked massive mudstone. Note branching of small tubes (white) in A that radiate from larger vertical tubes (appear as circles). Tubes (white) in B follow a polygonal pattern leaving undisturbed patches. Staple in A is 6 mm long, and staple in B is 7 mm long.

mudstones and, in some occurrences, are abundant. Remnant patches of laminated mudstone or ripple cross-laminated sandstone are common. In the Newark basin, a number of articulated reptile skeletons have been found in root-disrupted massive mudstones.

Root-disrupted massive mudstones occur in two common associations: (1) overlying and laterally equivalent to burrowed massive mudstone (Fig. 10-2, sequences 5 and 6); and (2) overlying and grading up from mud-cracked massive mudstone (Fig. 10-2, sequences 3 and 4; Fig. 10-18). In the first case, the transition is gradual, resulting from an increase of root and carbonate nodule abundances. In the second case, the transition occurs by tubes first preferentially following crack polygons (Fig. 10-11B), then dominating the mudstone fabric (Fig. 10-11A).

The root-disrupted mudstones are formed in vegetated environments, including sheet-like flood plains or subaerially exposed lake deposits of a basin floor, river overbanks, or the margins of lakes. Some of the root-disrupted massive mudstone may represent purely destructive fabrics of pre-existing deposits, while others may represent aggradational deposits. The association of roots and carbonate nodules in a massive mudstone is commonly interpreted as an arid soil containing caliche (e.g., Hubert, 1977; Hubert et al., 1978, pp. 23 – 31; Blodgett, 1984), by analogy to Giles et al. (1966). Profiles of centimeter-scale, coalescing carbonate nodules, similar to those of Giles and co-workers, are commonly associated with sandstones and conglomerates, but carbonate nodules in most massive mudstones do not occur in vertical profiles and are not gradational to the larger nodules. The small nodules that do not occur in vertical profiles are similar to soil carbonates in monsoonal conditions, such as in India (Mermut and Dasog, 1986). The varieties of carbonate nodules may reflect different climates, soil drainage, or water chemistry. Some nodules may form during later diagenetic events, as evidence of syndepositional origin is lacking. Tangential clays lining root tubes and bowl-shaped slickenside planes in some deposits are also suggestive of soil development, but no systematic profiles of their distributions have been described.

Sand-patch massive mudstone

Sand-patch massive mudstone contains small (1 – 5 cm long), irregular pods of sandstone and siltstone having the following diagnostic characteristics: angular margins; internal, jagged, mud-filled cracks; internal zones of different grain sizes; and cuspate contacts with the surrounding mudstone (Figs. 10-12, 10-13). The irregular pods do not have ovate or arcuate cross sections like the burrow mottles they superficially resemble. The sand pods may have internal cross-laminae that are not oriented with respect to cross-laminae in adjacent pods. Sand-patch massive mudstone is associated with eolian sandstone cross-strata and meter-scale lenses (Fig. 10-15), evaporite molds, and discoidal crystals or nodules of gypsum (Fig. 10-13).

Sand-patch massive mudstone typically overlies irregular thin-bedded sandstone and mudstone layers (Fig. 10-2, sequence 2; Fig. 10-17). The sandstone layers may have ripple cross-lamination that is commonly distorted and layer boundaries are commonly wispy. The irregularly bedded sandstone layers of some cycles overlie laminated, mud-cracked shale which may contain fish fossils.

Hubert and Hyde (1982) interpreted the sand patches as eolian adhesion ripples. However, the sand patches more closely resemble fabrics produced in modern saline mudflats (Fig. 10-12B), where wind-blown and stream-deposited sand and silt trapped in surface irregularities
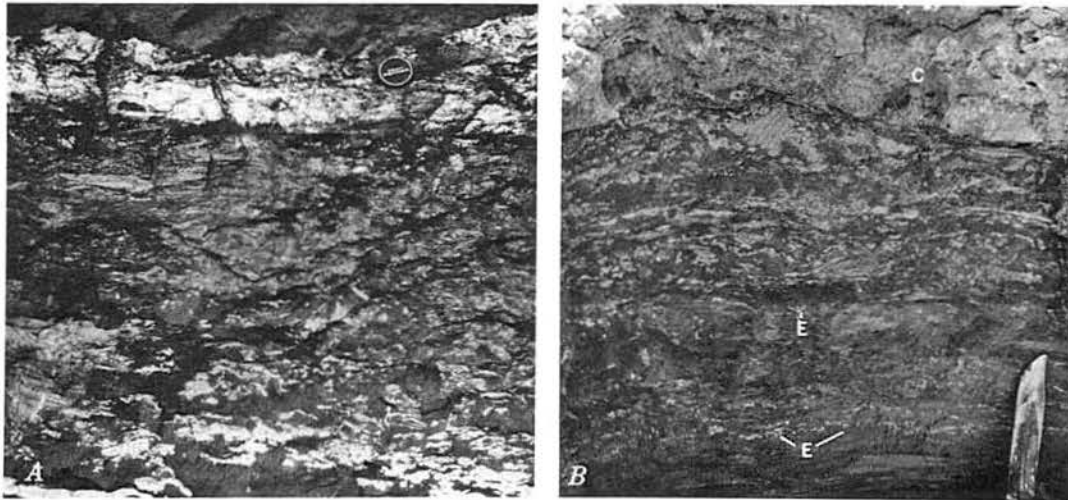
Fig. 10-12. Cross sections of (A) outcrop of sand-patch massive mudstone, Blomidon Formation, Fundy basin, Nova Scotia and (B) trench through an efflorescent halite crust (c) and underlying muds of saline mudflat in Saline Valley, California. Sand pods in B (light gray) are comprised of silt to coarse sand similar to the sediment between the surface irregularites of the efflorescent salt crust in Fig. 10-14. Some of the light-colored patches in B are anhedral blebs of finely crystalline gypsum and halite (E). Shape and composition of irregular sand pods in A (light gray) are similar to those in B. White patches in A are reduced zones that surround sand pods or irregular vugs, thought to represent dissolved evaporite minerals. Exposures shown in A and B are both about 40 cm high.
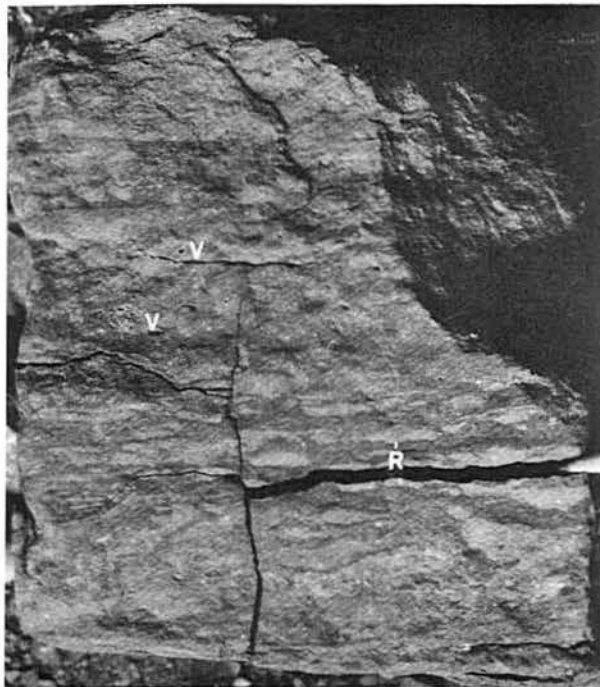

Fig. 10-13. Weathered surface showing cross section of sand-patch massive mudstone, Bigoudine Formation (Triassic), Argana basin, Morocco. Sand pods (light) are comprised of coarse silt- to granule-sized grains; mudstone (dark) is poorly sorted and sandy. Note irregular shapes of the sand pods and the cuspate contacts, as in basal contact of the deformed ripple structure near the middle of the sample (R). Black circles in upper third of sample are vugs (V), probably due to dissolution of anhedral crystal masses of evaporite minerals. Sample area shown is about 25 cm thick.

Fig. 10-14. Surface view of salt-encrusted saline mudflat at Saline Valley, California. Depressions between the ir-regularities of the efflorescent salt crust are filled with sand and silt (s) which forms lenses similar to those in Fig. 10-12B. Ruler is 30 cm long.

Fig. 10-15. Outcrop exposure of Blomidon Formation in the Fundy Basin, Nova Scotia. Middle, light-colored part of the exposure is dominated by 1 – 2-meter-thick alternations of sand-patch massive mudstone overlying distorted ripple beds. Upper and lower parts of exposure are comprised of 2 – 5-meter-thick cycles having mudcracked lacustrine shales at the base grading up into sand-patch massive mudstone. Cross-bedded lens at top of light-colored part of exposure is a small channel filled with fluvial and eolian sand (S). Exposure shown is 15 m thick.

of muddy efflorescent salt crusts (Fig. 10-14) are left as lags in massive mud when the salt dissolves (Smoot and Castens-Seidel, 1982). The cuspate margins of the modern sand pods reflect surface irregularities of the salt crust depressions, and their angular margins and internal cracks are probably due to deformation during multiple periods of dissolution. The distorted layers of ripple cross-laminated sandstone are similar to modern stream and shoreline deposits in the modern saline mud flats that are deformed by growth of thin efflorescent salt crusts.

Vertical sequences containing massive mudstones

The seven schematic sequences in Figure 10-2 illustrate some of the variability of the massive mudstone associations. Some of the variations occur within tens of meters in a stratigraphic succession (Figs. 10-15, 10-16). These sequences do not represent all variations, as can be seen in the measured sections (Figs. 10-17 – 10-20). We do not understand how much of the variability of cycle types is due to lateral facies changes. We have been able to correlate lateral changes in a few cases within the Newark and Hartford basins and suspect lateral changes in sequences, as shown in Figure 10-2.

Cycles similar to sequence 1 (Fig. 10-2) have been observed in the upper Lockatong Formation and lower Passaic Formation of Olsen (1980a) in the Newark basin (Katz, 1983) and in the lower East Berlin Formation in the Hartford basin (see Demicco and Kordesch, 1986). The cycles are typically 3 – 5 m thick. The thinner cycles have no laminated shale; the mudcracked massive mudstone directly overlies thin-bedded, mud-cracked, lacustrine mudstone or siltstone beds having polygonal curls. Thin cycles similar to sequence 1 also may occur

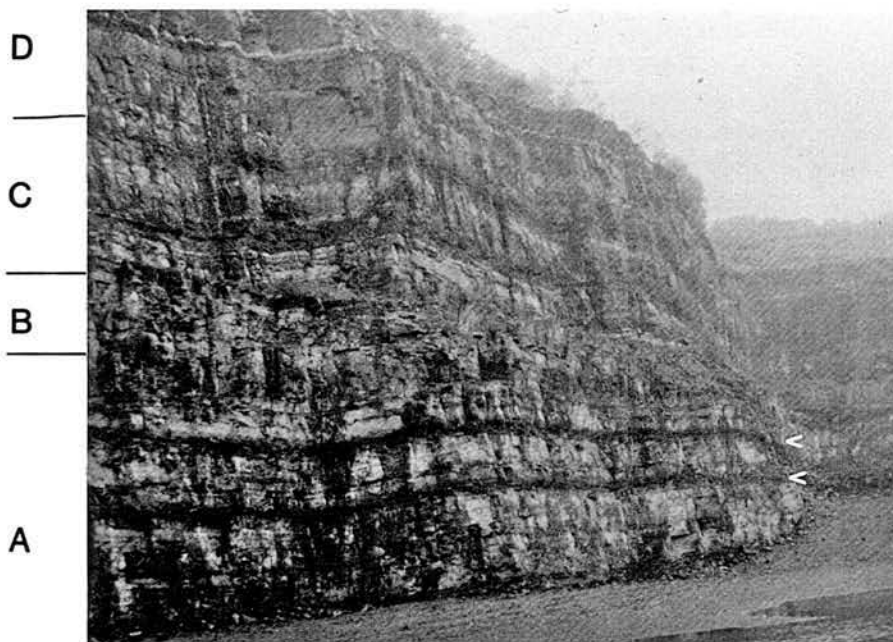Fig. 10-16. Quarry exposure of cyclic sequences in Lockatong Formation near Eureka, Pennsylvania. Sections labeled *A* and *C* are dominated by 5 – 7-m-thick cycles of organic-rich lacustrine shales grading upward to burrowed massive mudstone. Sections labeled *B* and *D* are dominated by mudcracked massive mudstone in 3 – 4-m-thick cycles. Two black shales marked by arrows are separated by 4 m, and the outcrop is 50 m high.

in the lowest portions of the Balls Bluff Siltstone in the Culpeper basin and in the Cow Branch Formation in the Danville basin.

Cycles similar to sequence 2 (Fig. 10-2) are illustrated in the stratigraphic section from the Blomidon Formation in the Fundy basin, Nova Scotia (Fig. 10-17). Cycles containing the sand-patch fabric have not been recognized in other Newark Supergroup basins but do occur in the Bigoudine Formation in the Argana basin in Morocco (Brown, 1980). Substantial thicknesses of laminated shale with fish fossils occur in some cycles in the Fundy basin. Cycles in the Argana basin may have up to a meter of laminated black shale at the base.

The stratigraphic section from the Balls Bluff Siltstone at Culpeper, Virginia (Fig. 10-18) illustrates some of the variability of sequence 3 (Fig. 10-2). These variations include cycles having well-developed lake laminites (cycles 3, 4, 5) and cycles having mud-cracked silt beds at the base (cycles 1, 2). Cycles with similar transitions from mud-cracked massive mudstone to root-disrupted massive mudstone occur in the Lockatong and Passaic Formations in the Newark basin (Olsen, 1980b), in the Cow Branch Formation in the Danville basin, and in the Gettysburg Formation in the Gettysburg basin. The cycles may occur in the Portland Formation in the Hartford basin and in the Boonton Formation in the Newark basin. Sequence
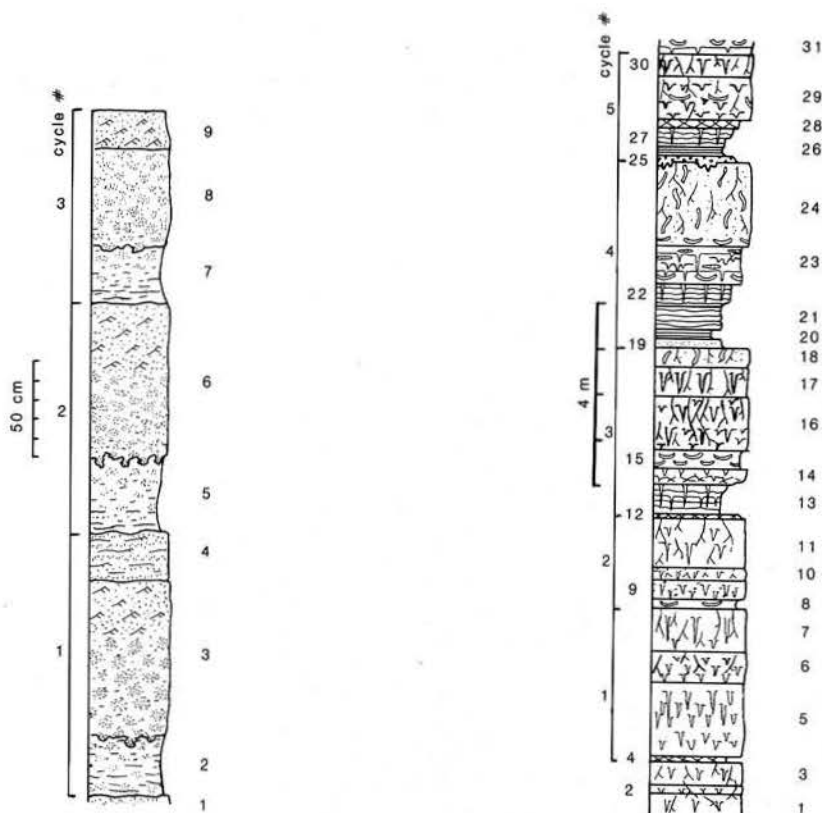

Fig. 10-17. Stratigraphic section of Blomidon Formation at Blomidon Park, Nova Scotia, Canada. See Appendix 1 for description of numbered lithologies.

Fig. 10-18. Stratigraphic section of Balls Bluff Siltstone in the Culpeper Crushed Stone Quarry, Stevensville, Virginia. See Appendix 1 for description of numbered lithologies.

4 cycles are the same as sequence 3 cycles, except for the evaporite crystal molds in the transition from thin-bedded mudstone having mud cracks to the brecciated portion of the mud-cracked massive mudstone. The evaporites appear to be syndepositional, as indicated by their unique position in the cycles and by their vertical change in character from large euhedral crystal shapes having growth orientation away from bedding planes, to large radial growth euhedral crystals restricted to mud cracks, to small anhedral crystals (Fig. 10-6). The sequence 4 type of cycles occurs associated with sequence 3 cycles in the Lockatong and Passaic Formations.

The stratigraphic section from the Sanford Formation in the Durham basin (Fig. 10-19) is comparable to sequence 5 (Fig. 10-2). The calcareous shale at the base (units 3 – 7) is fossiliferous (Olsen, 1977) but changes character laterally within the outcrop to poorly bedded mudstone having wide, deep mud cracks. This sequence may not be related to the rise and fall of a lake as the other sequences are, but may represent a small lake or pond on a fluvial flood plain. The sandstone immediately overlying the shale (units 9, 10) was probably deposited as a crevasse delta or as a distributary mouth bar. Sandstone layers overlying this sequence have sedimentary structures indicative of point bar deposits of a small meandering river (Smoot, 1985, fig. 2.1). Sequences of burrowed massive mudstone, containing *Scoyenia,* grading upward into root-disrupted massive mudstone in association with fluvial or deltaic sandstones, occur throughout the Sanford Formation in the Durham basin; in the
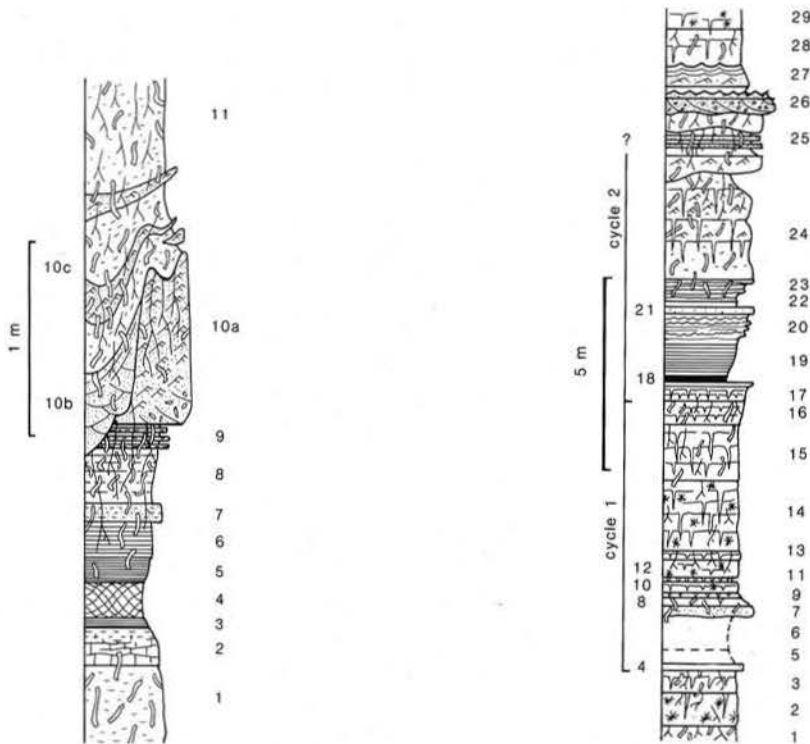

Fig. 10-19. Stratigraphic section of Sanford Formation in the Triangle Brick Quarry, Glenlee, North Carolina. See Appendix 1 for description of numbered lithologies.

Fig. 10-20. Stratigraphic section of Balls Bluff Siltstone along Cedar Run near Calverton, Virginia (see section C-1 of Gore, 1983). See Appendix 1 for description of numbered lithologies.

Midland Formation and portions of the Balls Bluff Siltstone in the Culpeper basin; in the Newfound Member and the upper part of the Falling Creek Member of the Doswell Formation in the Taylorsville basin; in the Gettysburg Formation in the Gettysburg basin; in the Stockton, Lockatong, Passaic, Feltville, and Towaco Formations in the Newark basin; in the Shuttle Meadow, East Berlin, and Portland Formations in the Hartford basin; and in the McCoy Brook Formation in the Fundy basin. Many of these occurrences form the upper parts of lake cycles and represent fluvial deposition after lake level fell.

The stratigraphic section from Cedar Run in the Ball Bluff Siltstone of the Culpeper basin (Fig. 10-20) includes lake sequences (cycles 1, 2) similar to sequence 6 (Fig. 10-2). Sequences where laminites grade into burrowed massive mudstone through loss of their layering then into root-disrupted massive mudstone are also found in the Midland and Turkey Run Formations in the Culpeper basin; in the Falling Creek Member of the Doswell Formation in the Taylorsville basin; in the Passaic, Feltville, Towaco, and Boonton Formations in the Newark basin; and in the Shuttle Meadow, East Berlin, and Portland Formations in the Hartford basin. Red root-disrupted massive mudstones in the Cedar Run section have evaporite crystal molds that are apparently randomly distributed in discrete layers. The crystal casts may be an early diagenetic feature. The root-disrupted massive mudstone having evaporite crystal molds also were observed in the Passaic Formation and in the Portland Formation.

The Lockatong Formation at Eureka Quarry (Fig. 10-16) is an example of sequence 7 (Fig. 10-2), although some cycles have a breccia fabric at the top. Sequences in which the cycle tops are burrowed massive mudstone having no root casts and only a few deep mud cracks are common throughout the lower Lockatong, in the Cumnock Formation of the Deep River basin, and in shale units of the lower barren beds of the Richmond basin.

Discussion

Our interpretations of the massive mudstones, based on comparisons with modern deposits, suggest that the upper portions of lacustrine cycles can be ranked into those deposited under the driest conditions to those deposited under the wettest conditions (Fig. 10-2). If, as we believe, the upper parts of the cycles represent the driest portions of climatic cycles, we have an independant measure of how dry conditions became in different stratigraphic units and in different basins. This breakdown can supplement other indicators of climatic variation, such as abundance and thickness lacustrine shale units (Van Houten, 1962, 1964; Olsen, 1984), presence of eolian sandstone units and evaporites (Hubert et al., 1978; Hubert and Mertz, 1980), or fossil assemblages, such as pollen (Cornet, 1977). The evaluation of massive mudstone may be more sensitive than these other approaches due to the abundance of massive mudstone in the basins and their rapid stratigraphic changes.

Mud-cracked massive mudstone (sequence 1) and sand-patch massive mudstone (sequence 2) are interpreted as deposits formed under relatively arid basin-floor conditions. A thick accumulation of the crumb fabric in a playa setting requires prolonged periods of total dryness punctuated by brief flooding events every several years, while the salt crusts envisioned for the sand-patch fabric require evaporation of a shallow, persistent, saline groundwater table. The latter conditions are best met by orographic deserts in areas of relatively high precipitation, such as the block-fault basins of the northern Basin and Range of North America or the rift basins in semitropical East Africa. Sequences containing burrowed and root-disrupted massive mudstones represent wetter depositional conditions than those having only the mud-cracked or sand-patch massive mudstones. The root-disrupted massive mudstones

at the tops of sequences 3 and 4 overlie mud-cracked massive mudstone, this change of character indicates a shift from conditions too dry to support vegetation to conditions having enough moisture to allow root penetration. If the burrows in sequences 5, 6, and 7 were made by crayfish-like crustaceans and/or worms, they indicate that the sediments were at least moist, if not water-saturated. Fluvial sandstones, mud cracks, and root structures in sequence 5 indicate that the sediments were deposited subaerially or in shallow-water conditions. Sequence 6 is mostly lacustrine and has mud cracks only at the top within root-disrupted massive mudstone. The burrowed massive mudstone overlying the lake deposits in sequence 7 contains no mud cracks or roots, although large, deep mud cracks at the top indicate some subaerial exposure.

Sand-patch massive mudstone is apparently restricted to the Fundy basin in the Newark Supergroup, and mud-cracked massive mudstone occurs within several stratigraphic units in the Newark, Hartford, Culpeper, and Danville basins but has not been observed in the Durham, Sanford, Wadesboro, Richmond, or Taylorsville basins. In the latter five basins, the burrowed or root-disrupted massive mudstones are the dominant varieties. This presence or absence change from drier massive mudstone textures in the northern basins to wetter massive mudstones in the southern basins supports the hypothesis that the sediments preserved in the exposed Newark basins reflect increasing aridity towards the north, due to the change in paleolatitude (Hubert et al., 1978). A major problem with this interpretation is that the burrowed and root-disrupted massive mudstones are present in all of the basins, including the Fundy basin. The presence of both wet and dry mudstone fabrics at the tops of cycles suggests that the northern basins may have been an unstable climatic area subject to variations in aridity over time.

The changes from dry massive mudstones to wet massive mudstones appear to be at least in part stratigraphically controlled, while lateral facies changes also affect the occurrences of mudstone types. Some of the possible coeval lateral relationships of massive mudstone sequences within a basin are shown in Figure 10-2. Based on the stratigraphic correlations of Olsen (1984, pp. 85 and 115−119) in the Newark basin, the equivalence of more basinal deposits similar to sequence 3 to deposits like sequence 5, and of sequences 4 to 3 and 7 to 5 were established. The other lateral relationships shown in Figure 10-2 are suggested by less well-constrained correlations in other basins. Stratigraphic changes in the depositional conditions from drier to wetter settings within the basins are indicated by the transition from abundant sequences with wet massive mudstones in the Carnian of the northern basins to sequences dominated by dry massive mudstones in the Norian. A change to more wet sequences occurs near the Triassic−Jurassic boundary. These stratigraphic changes are consistent with climatic variations inferred by Cornet (1977, pp. 61−71) on the basis of pollen data. The comparability of the two independent techniques suggests that we may be able to apply our criteria for a paleoclimatic chronostratigraphic correlation of much finer divisions among all of the basins.

The climatic implications of the massive mudstone textures suggest possible application as constraints for stratigraphic reconstructions. Mudstone cycles dominated by dry characteristics (i.e., sand-patch or mud-cracked massive mudstone textures) may be laterally correlated to sandstones and conglomerates also reflecting dry conditions (i.e., debris flows and sheet floods); mudstone cycles dominated by wet characteristics (burrow and root-disrupted massive mudstone textures) may be similarly correlated to the sandstones and conglomerates reflecting deposition under sustained higher discharges (i.e., braided or meandering river deposits having large-scale cross-bedding). There are obvious problems with

distinguishing between changes in fluvial style due to climate and those due to tectonic influence (see LeTourneau, 1985), such as changes in stream drainage areas or the location of base level in basins. By analogy to modern closed basins, however, we know there is a link between fluvial style and the deposits in the central basin (Smoot, 1985), and the evidence for rhythmic changes in lake level is more consistent with climatic controls than with tectonic controls (Olsen, 1986). More information is needed concerning the lateral variability of massive mudstone fabrics. We also need to determine if there are subtle differences within a specific type of massive mudstone that may indicate a more complex breakdown of mudstone types or stronger affinities between the different types. Even if the variations in massive mudstones ultimately prove to have limited climatic or stratigraphic utility, our understanding of the depositional environments of the Newark Supergroup can be improved by recognition of their differences.

Appendix 1: Descriptions of lithologies in measured sections in Figures 10-17 – 10-20.

A. *Blomidon Formation* (Fig. 10-17)
1. Brown muddy sandstone having irregular wispy lenticular beds (deformed ripples?).
2. Red mudstone having irregular green mottles and wispy lenses of sandstone. Thickness – 30 cm.
3. Brown sandy mudstone having sand-patch fabric grading up into muddy sandstone with irregular ripple cross-laminated lenses. Thickness – 80 cm.
4. Irregular, lenticular thin beds of brown sandstone and red mudstone defining deformed ripples. Layer boundaries are indistinct. Thickness – 25 cm.
5. Red mudstone having irregular green mottles and wispy lenses of sandstone. Thickness – 40 cm.
6. Brown sandy mudstone having sand-patch fabric grading up into muddy sandstone having irregular ripple cross-laminated lenses. Thickness – 80 cm.
7. Red mudstone having irregular green mottles and wispy lenses of sandstone. Thickness – 30 cm.
8. Brown sandy mudstone having sand-patch fabric. Thickness – 50 cm.
9. Brown muddy sandstone having irregular ripple cross-laminated lenses. Thickness – 20 cm.

B. *Balls Bluff Siltstone* (Fig. 10-18)
1. Red silty mudstone having abundant root casts filled with tan weathering dolomitic cement. Large narrow cracks are also partially filled with dolomitic cement. Thickness – 45 cm.
2. Red silty mudstone having calcite-filled root casts and spherical vugs. Roots appear to follow polygonal crack pattern. Thickness – 25 cm.
3. Red silty mudstone having abundant root casts and long narrow cracks similar to unit 1. Density of root casts and diameters of tubes appear to increase towards the top. Thickness – 40 cm.
4. Greenish-gray, shaley mudstone broken into a breccia fabric having red, silty mudstone crack fillings. Thickness – 15 cm.
5. Red silty mudstone having crumb fabric. Vesicle vugs are filled with calcite cement. Thickness – 200 cm.
6. Red mudstone having root casts that follow polygons. Root casts are filled with dolomitic cement near the base and calcite-cement in the upper 40 cm. Root casts are more abundant towards the top as mud cracks are less abundant. Thickness – 50 cm.
7. Red silty mudstone having abundant root casts and long narrow cracks similar to those of unit 3. Thickness – 70 cm.
8. Thin beds of tan-weathering dolomite-cemented siltstone broken into polygonal curls separated by red silty mudstone having abundant calcite and dolomite cement-filled vesicular vugs. Siltstone layers commonly have scoured basal contacts and may have internal oscillatory ripple cross-lamination. Lower siltstone beds are less curled and less brecciated than the upper siltstone layers. Thickness – 20 cm.
9. Red silty mudstone having crumb fabric, as in unit 5. Tan-weathering siltstone curls are very brecciated and widely separated. Thickness – 45 cm.
10. Red silty mudstone having root casts following polygons as in unit 6. Thickness – 25 cm.
11. Red silty mudstone having abundant root casts and long narrow cracks, as in unit 3. Upper 30 cm is gray colored, grading downward to the red. Thickness – 100 cm.

12. Tan-weathering dolomitic siltstone broken into polygonal curls, as in unit 8 but surrounded by gray mudstone having dolomite-filled vesicular vugs. The curls are flatter and less brecciated towards the top. Thickness — 5 cm.

13. Gray mudstone having thin beds of coarse siltstone, disrupted by 10–20-cm-deep polygonal cracks. Siltstone layers have oscillatory ripple cross-lamination. Mud cracks are more closely spaced and shallower upward, and siltstone layers have more basal scour. Thickness — 75 cm.

14. Gray mudstone having siltstone interbeds as below, broken into breccia by polygonal mud cracks. Grades upward in gray silty mudstone having crumb fabric and dolomite-filled vesicular vugs. Thickness — 35 cm.

15. Tan-weathering dolomitic siltstone broken into polygonal curls, as in unit 8, and surrounded by gray mudstone, as in unit 12. Silt curls are more brecciated upward, as in unit 8, and have about 3 cm of crumb fabric at the top. Lowest siltstone curls are also more brecciated. Thickness — 35 cm.

16. Gray silty mudstone having root casts following polygons and becoming more abundant upward, as in unit 6. Thickness — 110 cm.

17. Gray silty mudstone having abundant root casts and long mud cracks, as in unit 1. Sulfide minerals become more abundant towards the top. Thickness — 75 cm.

18. Tan-weathering, black sandy mudstone having abundant root casts and sulfide minerals. Nodular dolomite concretions are common. Widely spaced, long mud cracks still occur. Thickness — 35 cm.

19. Tan-weathering, sandstone having abundant black shale intraclasts. Basal contact is erosional into a sheared black shale, and the sandstone is coarse-tail graded. The sandstone layer is 0–7 cm thick. Thickness — 10 cm.

20. Black organic-rich shale having flat parting surfaces. Appears to have fine pinch-and-swell lamination. Irregular granule-sized lumps on bedding planes may be pellets or casts of shells. Thickness — 20 cm.

21. Black organic-rich shale having pinch-and-swell to lenticular siltstone laminae. Siltstone beds are thicker and more lenticular upwards. The thicker layers have oscillatory ripple cross-lamination. Small load casts are common. Thickness — 80 cm.

22. Gray mudstone having coarse siltstone thin beds and polygonal cracks, as in unit 13. Mud cracks also become more abundant, as in unit 13. Thickness — 50 cm.

23. Tan-weathering sandstone having gray silty mudstone interbeds. Basal siltstone layers are broken into polygonal curls grading upward into irregular lenticular sands having mudstone partings broken into small polygonal cracks. Dinosaur tracks occur on the mudstone partings. Irregular nodular patches of dolomitic cement are common. Thickness — 60 cm.

24. Tan-weathering, black sandy mudstone having abundant root casts and sulfide minerals. Long mud cracks are more common at the base, and dolomite and epidote nodules are common at the top. Uppermost surface is very hummocky and has large dinosaur tracks (a possible wallow). Tracks are less abundant and root structures are smaller to the east. Thickness — 170 cm.

25. Oolitic calcarenite having angular stromatolitic clasts. The layer is very lenticular, apparently filling irregularites in the lower layer. The calcarenite is very poorly sorted and has abundant sulfide minerals. Thickness — 0–20 cm.

26. Black organic-rich shale having pinch-and-swell to lenticular silt laminae. Basal several centimeters have polygonal cracks where directly overlying unit 24. Very similar to unit 21. Thickness — 20 cm.

27. Gray mudstone having coarse siltstone thin beds and polygonal cracks, as in unit 13. Thickness — 45 cm.

28. Gray mudstone as below, broken into a breccia surrounded by red silty mudstone. Some of the silt layers near the base are curled into polygons. Thickness — 20 cm.

29. Red silty mudstone having root casts that follow polygons and become more abundant upwards, as in unit 6. A layer of silt curls occurs about midway, and the lowest part may consist of crumb fabric without roots. Thickness — 80 cm.

30. Red silty mudstone having abundant root casts and long cracks, as unit in unit 1. Thickness — 30 cm.

31. Tan dolomitic siltstone broken into polygonal curls, as in unit 8. Thickness — 50 cm.

C. *Sanford Formation* (Fig. 10-19)

1. Green, mottled blocky siltstone having abundant burrows. Thickness — 250 cm.

2. Gray-green blocky siltstone grading down into a crudely laminated limestone. Fish scales are common. Thickness — 20 cm.

3. Green and red claystone having fine lamination. *Cyzicus, Darwinula*, fish scales, and rare *Scoyenia*. Thickness — 5 cm.

4. Brown claystone, disrupted by small faults and containing abundant slickensides. Thickness — 15 cm.

5. Green and red claystone having thick lamination. Unionid and corbiculid clams, *Cyzicus, Darwinula*, crayfish,

Scoyenia, fish scales, and rare root structures. Thickness — 15 cm.

6. Green and red thin-bedded claystone. Root structures more abundant than below. Unionid and corbiculid clams, *Cyzicus, Darwinula, Scoyenia,* and fish scales. Thickness — 15 cm.

7. Green siltstone having *Scoyenia* burrows. Thickness — 10 cm.

8. Red and green claystone having *Scoyenia* burrows and root structures. *Cyzicus, Darwinula,* and fish scales. Thickness — 28 cm.

9. Three, thin green siltstone beds separated by red and green claystone. Root structures and *Socyenia* burrows are abundant. These layers are truncated by the erosional base of unit 10. Thickness — 12 cm.

10. White to tan sandstone with red siltstone interbeds near top. 10a sandstone is comprised of climbing ripple cross-lamination or low-angle tabular sets overlying a flat contact. The basal part is rich in mud clasts, and the upper contact is convex, changing the thickness up to 30 cm. 10b sandstone is scoured into the underlying strata, it is internally trough cross-bedded, and the underlying claystones are mud-cracked. The sandstone is disrupted by *Scoyenia* burrows and root structures. 10c thin sandstone beds have abundant burrow and root structures and little internal stratification. Thickness — 110 cm.

11. Red, blocky, silty mudstone having abundant root structures and *Scoyenia* burrows. Thickness — 40 cm.

D. *Balls Bluff Siltstone* (Fig. 10-20)

1. Red silty mudstone having poorly defined sandstone layers disrupted by abundant root structures and other tubes, which are possibly burrows. Long, narrow mud cracks are common. Thickness — 40 cm.

2. Red silty mudstone like unit 1 but has calcite-filled molds of subhedral crystals (evaporites?). Thickness — 85 cm.

3. Red silty mudstone like unit 1. A nodular carbonate 5 cm long at the upper contact may be a tufa concretion. Thickness — 55 cm.

4. Gray, very fine-grained sandstone having shale partings. Sandstone thin beds pinch and swell with indistinct cross-laminae, and shale partings have internal pinch-and-swell lamination. Small burrows disrupt the fabric. Thickness — 20 cm.

5. Covered interval is mostly gray shale chips. Thickness — 30 cm.

6. Covered interval is mostly red silstone chips. Thickness — 100 cm.

7. Red fine-grained sandstone having low-angle climbing ripple cross-lamination. *Scoyenia* burrrows near the top. Thickness — 20 cm.

8. Thin beds to thick laminae of red, very fine-grained sandstone and shale. Sandstone layers are ripple cross-laminated and have soft-sediment deformation structures. *Scoyenia* burrows are common, and small cracks occur at the top. A large linear disruption feature may be a large crack or a tap root. Thickness — 15 cm.

9. Red silty mudstone having a very fine-grained sandstone layer. Root structures and small cracks making a breccia-like pattern are common. A large crack cuts the whole layer. Thickness — 10 cm.

10. Red silty mudstone having numerous root structures. Small polygonal cracks occur in claystone partings particularly near the top of the unit. Thickness — 30 cm.

11. Red silty mudstone in irregular thick laminae having claystone partings. Lower layers are disrupted by large polygons (25- to 30-cm polygons), and upper layers have smaller polygons and more tubes (roots?). Thickness — 10 cm.

12. Red silty mudstone having abundant root structures and remnant patches of sandstone layers. Some possible calcite-filled crystal molds. Thickness — 45 cm.

13. Red muddy siltstone having abundant root structures and patches of remnant sandstone layers. Large complex mudcracks cut through the layer. Thickness — 20 cm.

14. Red silty mudstone having root structures, long cracks, and calcite-filled crystal structures, as in unit 2. Thickness — 190 cm.

15. Red silty mudstone like unit 1. Thickness — 140 cm.

16. Red muddy siltstone and very fine-grained sandstone having abundant root structures and other tubes. Lower part has carbonate nodules, and the upper part has claystone partings and small polygonal cracks. Large carbonate nodules in the uppermost part may be cement concretions. Thickness — 65 cm.

17. Gray, thin-bedded to thick-laminated, very fine-grained sandstone having shaly partings. Sandstone layers pinch and swell with oscillatory ripple cross-lamination. Mud crack polygons in shale partings are progressively greater in diameter and deeper penetrating towards the top of the unit. Tubes are less abundant towards the top. Thickness — 40 cm.

18. Black, finely laminated calcareous shale overlying a calcareous sandstone having oscillatory ripple cross-lamination, and underlying an intraclast limestone conglomerate layer. The black shale over the conglomerate

layer has a fine pinch-and-swell lamination. Thickness — 15 cm.

19. Dark gray shale having a thicker pinch-and-swell lamination than below. Some layers appear to be more poorly bedded, but that may be due to weathering. Thickness — 90 cm.

20. Greenish-gray shale having thick lamination that is less well defined than below (burrowing?). Pinch-and-swell sandstone laminae increase upward to lenticular sandstone thin beds having oscillatory ripple cross-laminae and load structures. Thickness — 75 cm.

21. Red, fine-grained, thin-bedded sandstone having oscillatory ripple cross-lamination and shaley partings. Some sandstone layers have load structures at their base. Thickness — 10 cm.

22. Dark gray shale that is sandy near the base and has progressively thinner pinch-and-swell laminae grading into fine laminae with lenses of ostracode shells above it. Uppermost part is sandy and has progressively thicker laminae, which are more lenticular, towards the top contact. The gray color grades to red towards the top. Thickness — 20 cm.

23. Red muddy siltstone to muddy sandstone in thick laminae to thin beds having shaly partings. Finer-grained layers have pinch-and-swell lamination and isolated ripple structures. The coarser layers are graded beds of climbing ripples having abundant load structures. Many layers appear diffuse, apparently due to bioturbation (burrows?). Thickness — 60 cm.

24. Red sandy siltstones having fine- to medium-grained sandstone interbeds 20–30 cm thick. Siltstone intervals are very burrowed and have remnant patches of sandstone layers; sandstone layers have low-angle climbing ripples and more burrows at their tops. All layers are cut by large cracks up to 70 cm in diameter and 60 cm deep. Root structures occur near the top. Thickness — 285 cm.

25. Red, medium- to fine-grained sandstone beds having sharp basal contacts grading to sandy siltstone. Some sandstone layers have vague flat lamination and ripple cross-lamination, while siltstone intervals have only patches of layering. Tubes are abundant, including *Scoyenia* burrows and calcite-filled root structures. Carbonate nodules are common towards the top. Sharp bases are irregular due to scour or loading. Thickness — 145 cm.

26. Red sandstone comprised of well-rounded carbonate granules forming tabular foresets. The basal contact is flat and sharp. The carbonate grains are like the nodules in the underlying layers. Thickness — 35 cm.

27. Red, medium-grained sandstone having carbonate granules, wavy parting, and possible internal cross-lamination. It is overlain by two graded layers of fine-grained sandstone having low-angle climbing ripples grading to high-angle climbing ripples. *Scoyenia* burrows and other tubes dominate the tops of the graded beds. Thickness — 80 cm.

28. Red muddy siltstone having disrupted layers of very fine sandstone with internal ripple cross-lamination, grading up to silty mudstone with patches of remnant layering. Root structures and possible burrows are abundant. The upper part has long, narrow cracks. Thickness — 95 cm.

29. Red silty mudstone having root structures, long cracks, and calcite-filled crystal molds, as unit 2. Thickness — more than 100 cm.

References

Bain, G.L. and Harvey, B.W., 1977. Field guide to the geology of the Durham Triassic basin. Carol. Geol. Soc., 40th Anniversary Meeting, Raleigh, North Carolina Department of Natural Resources and Community Development, Geologic Survey Section, 83 pp.

Blodgett, R.H., 1984. Nonmarine depositional environments and paleosol development in the Upper Triassic Dolores Formation, southwestern Colorado. In: Brew D.C. (Editor), Field Trip Guidebook for the 37th Annual Meeting, Rocky Mountain Section, Geol. Soc. Am., pp. 46–92.

Bown, T.M. and Kraus, M.J., 1981. Lower Eocene alluvial paleosols (Willwood Formation, northwest Wyoming, U.S.A.) and their significance for paleoecology, paleoclimatology, and basin analysis. Paleogeogr., Paleoclimatol., Paleoecol., 34: 1–30.

Brown, R.H., 1980. Triassic rocks of Argana Valley, southern Morocco, and their regional structural implications. Bull., Am. Assoc. Pet. Geol. 64: 988–1003.

Cornet, B., 1977. The palynostratigraphy and age of the Newark Supergroup. Ph.D. thesis, Pennsylvania State University, State College, 506 pp. (unpubl.).

Demicco, R.V. and Kordesch, E.G., 1986. Facies sequences of a semi-arid closed bain: the Lower Jurassic East Berlin Formation of the Hartford Basin, New England, U.S.A. Sedimentology, 33: 107–118.

Frey, R.W., Pemberton, S.G. and Fagerstrom, J.A., 1984. Morphological, ethological, and environmental significance of the ichnogenera *Scoyenia* and *Ancorichnus*. J. Paleontol., 58: 511–528.

Froelich, A.J. and Olsen, P.E., 1985. Newark Supergroup, a revision of the Newark Group in eastern North America. In: G.R. Robinson and A.J. Froelich (Editors), Proceedings of the Second U.S. Geological Survey Workshop on the Early Mesozoic Basins of the Eastern United States. U.S. Geol. Surv., Circ., 946: 1–3.

Giles, L.H., Peterson, F.F. and Grossman, R.B., 1966. Morphological and genetic sequences of carbonate accumulation in desert soils. Soil Sci., 101: 347–360.

Gore, P.J.W., 1983. Sedimentology and invertebrate paleontology of Triassic and Jurassic lacustrine deposits, Culpeper basin, northern Virginia. Ph.D. thesis, George Washington University, Washington D.C., 356 pp. (unpubl.).

Gore, P.J.W., 1986. Depositional framework of a Triassic rift basin: the Durham and Sanford sub-basins of the Deep River basin, North Carolina. In: D.A. Textoris (Editor), Society of Economic Paleontologists and Mineralogists Field Guidebooks, Southeastern United States, 3rd Annual Midyear Meeting, Raleigh, N.C., pp. 53–115.

Gray, M.B., 1984. Slickensided soil fractures – Indicators of strain and deformation processes in the Bloomsburg Formation, central Pennsylvania. Geol. Soc. Am. Abstr. with Programs, 16: 19.

Hentz, T.F., 1985. Early Jurassic sedimentation of a rift-valley lake: Culpeper basin, northern Virginia. Geol. Soc. Am. Bull., 96: 92–107.

Hubert, J.F., 1977. Paleosol caliches in the New Haven Arkose, Connecticut: record of semiaridity in Late Triassic–Early Jurassic time. Geology, 5: 302–304.

Hubert, J.F. and Hyde, M.G., 1982. Sheetflow deposits of graded beds and mudstones on an alluvial sandflat-playa system: Upper Triassic Blomidon redbeds, St. Mary's Bay, Nova Scotia. Sedimentology, 29: 457–474.

Hubert, J.F. and Mertz, K.A., 1980. Eolian dune field of Late Triassic age, Fundy basin, Nova Scotia. Geology, 8: 516–519.

Hubert, J.F., Reed, A.A. and Carey, P.J., 1976. Paleogeography of the East Berlin Formation, Newark Group, Connecticut Valley. Am. J. Sci., 276: 1183–1207.

Hubert, J.F., Reed, A.A., Dowdall, W.L. and Gilchrist, J.M., 1978. Guide to the redbeds of central Connecticut. State Geologic and Natural History Survey of Connecticut, Guidebook 4, 129 pp.

Katz, S.B., 1983. Sedimentary features and soil-like fabrics in chemical cycles of the Lockatong Formation, Newark Supergroup (Late Triassic), New Jersey and Pennsylvania. M.S. thesis, State University of New York at Stony Brook, Stony Brook, NY, 134 pp. (unpubl.).

LeTourneau, P.M., 1985. Alluvial fan development in the Lower Jurassic Portland Formation, central Connecticut – Implications for tectonics and climate. In: G.R. Robinson and A.J. Froelich (Editors), Proceedings of the Second U.S. Geological Survey Workshop on the Early Mesozoic Basins of the Eastern United States. U.S. Geol. Surv., Circ., 946: 17–26.

Mermut, A.R. and Dasog, G.S., 1986. Nature and morphology of carbonate glaebules in some vertisols of India. Soil Sci. Am. J., 50: 382–391.

Olsen, P.E., 1977. Stop 11 – Triangle Brick Quarry. In: G.L. Bain and B.W. Harvey (Editors), Field Guide to the Geology of the Durham Basin. Carol. Geol. Soc., Fortieth Anniversary Meeting, pp. 59–60.

Olsen, P.E., 1980a. The latest Triassic and early Jurassic formations of the Newark basin (eastern North America, Newark Supergroup): Stratigraphy, structure, and correlation. N. J. Acad. Sci. Bull., 25: 25–51.

Olsen, P.E., 1980b. Fossil great lakes of the Newark Supergroup in New Jersey. In: W. Manspeizer (Editor), Field Studies in New Jersey: Geology and Guide to Field Trips. 52nd Annual Meeting of New York State Geological Assocation, Rutgers University, Newark, NJ, p. 352–398.

Olsen, P.E., 1984. Comparative paleolimnology of the Newark Supergroup – A study of ecosystem evolution. Ph.D. Thesis, Yale University, New Haven, CN, 726 pp. (unpubl.).

Olsen, P.E., 1985. Distribution of organic-matter-rich lacustrine rocks in the early Mesozoic Newark Supergroup. In: G.R. Robinson and A.J. Froelich (Editors), Proceedings of the Second U.S. Geological Survey Workshop on the Early Mesozoic Basins of the Eastern United States. U.S. Geol. Surv., Circ., 946: 61–64.

Olsen, P.E., 1986. A 40-million year record of Early Mesozoic orbital climate forcing. Science, 234: 842–848.

Reinemund, J.A., 1955. Geology of the Deep River coal field, North Carolina. U.S. Geol. Surv., Prof. Pap. 246, 159 pp.

Retallack, G.J., 1977. Triassic paleosols in the upper Narrabeen Group of New South Wales. I. Features of the paleosols. J. Geol. Soc. Aust., 32: 383–399.

Robbins, E.I., 1982. 'Fossil Lake Danville': The paleoecology of a Late Triassic ecosystem on the North Carolina–Virginia border. Ph.D. thesis, Pennsylvania State University, University Park, PA, 400 pp (unpubl.).

Smoot, J.P., 1981. Subaerial exposure criteria as seen in modern playa mudcracks (abs.). Bull., Am. Assoc. Pet. Geol., 65: 530.

Smoot, J.P., 1985. The closed-basin hypothesis and its use in facies analysis of the Newark Supergroup. In: G.R. Robinson and A.J. Froelich (Editors), Proceedings of the Second U.S. Geological Survey Workshop on the Early Mesozoic Basins of the Eastern United States. U.S. Geol. Surv., Circ., 946: 4–17.

Smoot, J.P. and Castens-Seidel, B., 1982. Sedimentary fabrics produced in playa sediments by efflorescent salt crusts: An explanation for 'adhesion ripples'. Abstracts of Papers, Int. Assoc. Sedimentol., 11th International Congress on Sedimentology, Hamilton, Ontario, p. 10.

Smoot, J.P. and Katz, S.B., 1982. Comparison of modern playa mudflat fabrics to cycles in the Triassic Lockatong Formation of New Jersey. Abstracts with Program, Northeastern – Southeastern Sections Geol. Soc. Am. Annu. Meet., Washington, D.C., p. 83.

Smoot, J.P. and Olsen, P.E., 1985. Massive mudstones in basin analysis and paleoclimatic interpretation of the Newark Supergroup. In: G.R. Robinson and A.J. Froelich (Editors), Proceedings of the Second U.S. Geological Survey Workshop on the Early Mesozoic Basins of the Eastern United States. U.S. Geol. Surv., Circ., 946: 29–33.

Van Houten, F.B., 1962. Cyclic sedimentation and the origin of analcime-rich upper Triassic Lockatong Formation, west-central New Jersey and adjacent Pennsylvania. Am. J. Sci., 260: 561–576.

Van Houten, F.B., 1964. Cyclic lacustrine sedimentation, Upper Triassic Lockatong Formation, central New Jersey and adjacent Pennsylvania. Kans., State Geol. Surv., Bull., 169: 497–531.

Van Houten, F.B., 1965. Crystal casts in Upper Triassic Lockatong and Brunswick Formations. Sedimentology, 4: 301–313.

Wells, R.F., 1977. Fresh water invertebrate living traces of the Mississippi alluvial valley near Baton Rouge, Louisiana. M.S. thesis, Louisiana State University, Baton Rouge, LA, 254 pp. (unpubl.).